ARMA 24–149

An Efficient Coupled Hydro-Geomechanical Model for Determination of Open Hole Extended Limit of Drilling Horizontal Wells in the Permian Basin by Using Developed Environmentally Friendly High Performance Water-Based Mud

Metwally, Mohamed
New Mexico Tech, Socorro, NM, USA
Gyimah, Emmanuel
University of North Dakota, Grand Forks, ND, USA
Koray, Abdul-Muaizz
New Mexico Tech, Socorro, NM, USA

ABSTRACT: Drilling horizontal and extended reach wells (ERW) has played critical role in enhancing well productivity, efficient reservoir drainage, and minimizing environmental impact. Despite the benefits, technical challenges like high torque, shale instability, and managing equivalent circulation density pose limitations to extending lateral sections. To address these issues, the paper proposes a high performance environmentally friendly water-based mud (WBM) with a friction reducer (FR) for ERW drilling in the shaly Wolfcamp and Spraberry formations within the Permian Basin. Objectives include developing a thermally stable WBM, inhibiting shale instability problems, mitigating barite sagging, being environmentally friendly and determining the maximum open hole extension limit for ERW using the hydraulic Herschel-Bulkley rheological model coupled with geomechanics. The laboratory analysis showcases the WBM's thermal stability, improved capability to inhibit shale, effectiveness in preventing bit balling, reduction in barite sagging, and mitigated adverse effects on the ecosystem. The hydraulic model utilizing the Herschel-Bulkley rheological model exhibits high accuracy in determining equivalent circulation density and annular pressure losses. The study introduces an innovative environmentally friendly WBM that not only minimizes pressure loss but also effectively addresses shale-related challenges, serving as a viable substitute for oil-based mud. It provides a reliable hydro-geomechanically model for predicting the increase in open hole extension limit within a safe mud weight window, thereby enhancing wellbore stability in the Permian Basin.

1. INTRODUCTION

In the context of oil and gas exploration, the stability of wellbores plays a pivotal role in determining the success and safety of drilling operations. The subsurface environment introduces formidable challenges, with diverse geological conditions that can significantly impact the structural integrity of a wellbore (Amanullah et al., 2018). Geomechanics analysis emerges as a crucial tool in this scenario, providing a systematic framework for comprehending and addressing the intricate interactions between the wellbore and the surrounding rock formations (Gyimah et al., 2023). This analysis integrates geological, geophysical, and engineering data to construct predictive models, offering insights into potential instabilities and guiding drilling operations. Key parameters such as in-situ stress conditions, rock strength, pore pressure, and the effects of drilling fluid circulation are carefully considered in geomechanics analysis for wellbore stability (Bagheri et al., 2021).

Geomechanics studies contribute valuable insights into the mechanical behavior of rock formations, facilitating the design of stable wellbores during drilling operations.

Accurate predictions of pore pressure and fracture pressure enable the identification and mitigation of drilling-related risks, including wellbore instability, kicks, and blowouts (Khaled et al., 2022). By anticipating pore and fracture pressures, drilling parameters like mud weight and rate of penetration can be optimized, leading to more efficient and cost-effective drilling. The proactive approach of geomechanics studies helps minimize non-productive time by averting unexpected wellbore stability issues and providing precise estimates of drilling parameters during operations.

The significance of geomechanics studies becomes even more pronounced when considering the drilling of extended reach wells (ERW). ERW, characterized by their substantial horizontal sections, introduce additional

challenges and complexities to wellbore stability (Zhang, 2019). In this context, geomechanics analysis plays a crucial role in determining open hole horizontal extension.

Horizontal and ERW drilling improves reservoir contact, resulting in heightened well productivity, particularly in reservoirs with low permeability (Li et al., 2023; Abdulaziz et al., 2018). Furthermore, this drilling approach reduces the necessity for multiple production wells, thereby minimizing the environmental impact. ERW also proves effectiveness in the efficient drainage of reservoirs and the mitigation of water coning, especially in scenarios characterized by thin oil columns and a robust active bottom-water drive (Okon, 2018).

ERW is defined when the ratio between Measured displacement (MD) and true vertical depth (TVD) is higher than 2.0 (Chen et al, 2017). Progress and improvements in horizontal drilling and completion technology have prompted operators to consistently seek the drilling of progressively longer lateral wells, aiming to increase hydrocarbon production. That is why, the range for extended-reach wells has been consistently widening in recent years, making it common to drill these wells with Measured Depth (MD) to True Vertical Depth (TVD) ratios exceeding 6.0 or horizontal lateral lengths surpassing 30,000 feet (Chamat et al., 2015).

However, the drilling of ERW faces constraints imposed by the extension limit of the horizontal section. The open hole extension limit of ERW is primarily influenced by formation fracture pressure, annular pressure losses, and the equivalent circulation density (ECD) of the drilling fluid (Metwally, 2024). In the realm of drilling fluids, operational challenges associated with ERW commonly involve issues such as hole cleaning, drilling within a narrow window between pore pressure and fracture pressure, shale instability problems, and torque and drag (Morrison et al., 2019). Addressing hole cleaning in ERW necessitates a higher circulation rate for improved efficiency, constrained by limitations in surface pumping capacity. However, this higher circulation rate can ultimately elevate ECD and restrict the open hole extension for ERW (Metwally et al., 2023). Consequently, the role of drilling fluid is crucial for the successful, safe, and economical drilling of ERW.

General speaking, oil based mud (OBM) is the preferred drilling fluid for horizontal wells and ER. OBM offers advantages in boosting the rate of penetration, improving the thermal stability of rheology, increasing lubricity, reducing friction coefficients in the drilling of horizontal wells and ERW, preventing swelling and dispersion of shale formations, and enhancing wellbore stabilization (Willis et al., 2018). However, the Environmental Protection Agency (EPA) has established regulations to limit the use of OBM due to its harmful impact on the environment. Additionally, OBM is associated with drawbacks such as high costs, disposal challenges, and health and safety concerns (Njuguna et al., 2022). Consequently, the escalating environmental legislations aimed at curbing OBM application in industries have led to the adoption of WBM as the most environmentally acceptable alternative.

The main problem in this paper is to formulate water-based mud (WBM) to be rheological stable with temperature, inhibit shale instability problem, be environmentally friendly, approach OBM performance, and able to reduce annular hydraulic friction pressure losses to extended open hole horizontal section limit. This mud formulation will be considered as high performance WBM. As the traditional WBM might not effectively prevent clay swelling and dispersion, which can result in wellbore instability, elevated torque and drag, and the possibility of encountering stuck pipe issues (Ma et al., 2022). Besides, shale formations generate sticky cuttings which can be adhesive to bit and bottom hole assembly and cause bit balling problem and inappropriate hole cleaning. Hence, drilling shale formation is another challenge to extend open hole ERW (Rady et al., 2024).

Moreover, hole cleaning is another major challenge in extending ERW. the main concern stems from the rise in annular pressure loss, which is linked to the need for a high circulation rate to improve hole cleaning. The increased pumping circulation rate induces turbulence, resulting in significant energy loss and heightened hydraulic friction (Ashena et al., 2021). Addressing the challenges posed by elevated frictional resistance and aiming to reduce pumping discharge, the petroleum industry is increasingly focusing on the utilization of friction reducer (FR) agents (Varnaseri and Peyghambarzadeh, 2020). Polymeric FRs, characterized by their high molecular weights, are linear polymers that can effectively reduce frictional pressure loss in turbulent flow when added in low concentrations (Aften and Watson, 2009).

Polymeric FR, in oil and gas industry, is currently essential additive in slickwater hydraulic fracture for minimizing friction loss, attaining a high drag reduction rate, and preventing formation damage (Ishak et al., 2023). There are numerous theories outlining the mechanism through which FR reduces hydraulic pressure loss. One notable theory suggests that FR holds the capability to transform turbulent flow into laminar flow by suppressing the formation of turbulent eddies, consequently leading to a reduced Reynolds number. In laboratory tests, the FRs have demonstrated a reduction in energy loss ranging from 20-80%, while in field applications, the reduction is observed to be between 30-90%, when compared to freshwater (Sun et al., 2010).

Another theory is based on Prandtl Mixing Length theory. Bradshaw (1974) introduced the Prandtl Mixing Length theory, categorizing the velocity profile within the pipe

into two layers without FR as shown in Fig.1a. The first layer, the viscous sub-layer at the pipe boundary, exhibits laminar flow with lower pressure loss. The second layer, the inertial layer at the pipe center, demonstrates turbulent flow with radial fluctuations, causing major pressure losses at higher flow rates. In contrast, with the presence of polymer FR, Bradshaw identified three layers in the cross-sectional velocity profile: the viscous sub-layer, inertial layer, and a newly introduced elastic buffer layer as demonstrated in Fig.1b. This buffer layer, formed between the viscous and inertial layers, experiences altered flow fluctuations as the FR uncoils and stretches, shifting them from radial to axial direction and inducing laminar flow (Metwally et al., 2022). The expansion of the buffer layer towards the pipe center leads to drag reduction by contracting the inertial layer.

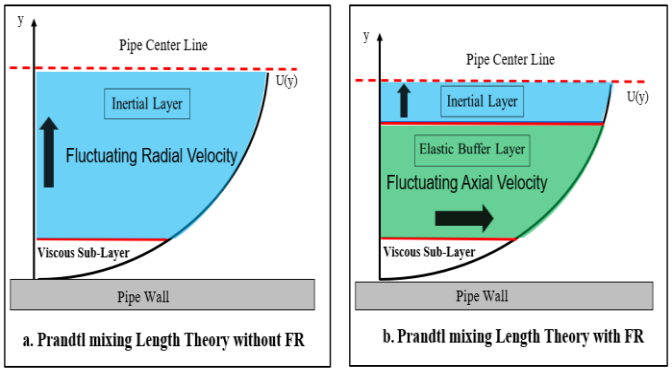

Fig. 1: Mechanism of friction reduction by using polymeric friction reducer (FR)

The field application of FR proved its capability to reduce the hydraulic pressure losses. There are many FRs available in oil and gas industry. One of them is polyacrylamide. Polyacrylamide is linear polymer that has high thermal stability, withstanding temperatures of up to approximately 400 °F, and it exhibits rapid decomposition beyond 550 °F. It offers superior drag reduction when compared to natural polymers (Xiong et al., 2018). Hence, polymeric polyacrylamide FR will be used in this research work due to its thermal stability. Adding FR to WBM could be potential to reduce hydraulic pressure loss at high circulation rate used to drill ERW. This may be help in elongation open hole horizontal ERW drilled specifically in the Permian Basin. The Permian basin, which located in eastern south New Mexico and West Texas, is treated as the largest province of oil and gas production in the U.S. with production beginning in 1921 (Ward et al, 1986). The Wolfcamp and Spraberry formations within the Permian Basin are acknowledged as the second-largest oil field globally, following the Ghawar field in Saudi Arabia. The trend of drilling horizontal and extended-reach wells in the Permian Basin is consistently on the rise (Sharma et al, 2019). From 2019 to 2022, there was an increase in average lateral length from 8,500 to 10,000 ft (Rassenfoss, 2022). The open hole lateral section in ERW within Permian basin depends mainly on operating mud windows between pore pressure and fracture pressure.

Hence, this paper introduces a novel approach by integrating geomechanics with mud hydraulics to determine the open-hole lateral horizontal section for ERW drilled in shale formations within the Permian Basin. Furthermore, the paper's innovation extends to the formulation of WBM with FR, aiming to create a high-performance environmentally friendly WBM that approaches OBM performance in drilling ERW in the Permian Basin.

2. METHODOLOGY

The methodology employed in this study encompasses a thorough exploration that combines experimental measurements and modeling to deepen the understanding within the specified research area. The experimental phase of the research strictly adhered to the guidelines and recommendations established by the American Petroleum Institute (API).

2.1 The Experimental Part

Conducting experimental work is crucial for the assessment of the developed high-performance WBM intended for drilling ERW in the shaly Spraberry and Wolfcamp formations within the Permian Basin. This assessment involves the examination of fluid rheology, barite sagging, and the shale inhibition characteristics of the formulated WBM, and evaluation of toxicity.

The fluid rheology analysis employed an OFITE 900 viscometer, which automatically measured shear stress across various shear speeds at different temperatures up to 200°F and ambient pressure. To simulate the conditions within the well, the OFITE Roller oven, equipped with five rollers, was utilized, allowing for aging under static or dynamic conditions at temperatures ranging from ambient to 600°F.

Various techniques are employed to assess the effectiveness of shale inhibitors in water-based muds (WBM) for shale inhibition purposes. These techniques encompass zeta potential, linear swelling test, hot rolling dispersion test, capillary suction test, methylene blue test, contact angle and scanning electron microscope (Ahmed et al., 2019). This study specifically utilized shale dispersion test, accretion test, and contact angle to investigate shale inhibition. The shale dispersion test, also referred to as the cutting dispersion test, involves grinding and sieving clay cuttings through 20-30 mesh screens. The sieved clay cuttings are then combined with the formulated drilling fluid in an aging cell within a roller oven for 16 hours. Subsequently, the shale cuttings are washed and recovered using a 50-mesh sieve, followed by a 3-hour heating process in the roller oven to ensure complete water evaporation. The recovered shale weight, compared to the original shale weight, indicates the shale

recovery percentage (Eq.1). A higher shale recovery percentage implies a more effective shale fluid inhibitor (Jain et al., 2015)

$$\text{Shale Recovery} = \frac{\text{weight of dry recovered shale cuttings}}{\text{Initial weight of shale cuttings}} \quad (1)$$

Accretion tests have been widely employed to investigate the propensity of clay to adhere to the bit and bottom hole assembly when exposed to various drilling fluids. This method is relatively straightforward and cost-effective. The laboratory-based accretion test involves utilizing a steel bar and a jar. The procedure commences by placing a clean hollow steel bar into a jar containing one barrel of drilling fluid. Subsequently, a specific weight (W_1) of ¼ inch bentonite tablets, representing shale cuttings with high shale swelling and adhesion tendency, are added. The jar is then sealed and horizontally positioned in a roller oven for 30 minutes at 120 ºF. Following this interval, the bar is extracted from the jar, and a qualitative analysis of the accreted bar is documented through photography. The adhered solids are subsequently removed from the steel bar, dried in an oven for three hours at 240° F, and their weight (W_2) is measured. The accretion percentage is computed using Eq. 1 (May et al., 2022).

$$\text{Accretion}(\%) = \frac{W_2}{\left[\frac{(100 - M)}{100}\right] \times W_1} \times 100 \quad (2)$$

Where:
M: Moisture content of unexposed bentonite tablets.
W_1: Initial weight of the shale cuttings added to the jar.
W_2: Weight of adhered shale cuttings after being dried.

The third method to evaluate shale inhibition in this study is the contact angle. A goniometer is an apparatus equipped with a high-speed camera designed to measure the contact angle between a water droplet and the clay surface. This angle serves as an indicator of shale surface wettability and can reveal alterations in wettability. In this study, shale cuttings were submerged in various formulated drilling fluids for 24 hours. Subsequently, the recovered shale underwent a drying process in a roller at 200°F for 4 hours. A micro syringe was then employed to apply a fixed volume of deionized water (5 µL) on the dry shale's flat surface. Then the contact angle will be measured by high resolution camera in the goniometer device. A small value of the measured contact angle suggests hydrophilicity of the shale surface, while an increasing contact angle signifies a shift towards reduced hydrophilicity and increased hydrophobicity (Murtaza et al., 2020).

The Viscometer Sag Shoe Test (VSST) serves as a predictive measure for the formulated WBM capability to suspend weighting materials and minimize the occurrence of barite sagging (Zamora et al., 2004). The inclined surface of the sag shoe is intentionally designed to expedite the settling of weighting materials, concentrating them in the collection well. The VSST procedure involves placing the sag shoe within the viscometer plate, adding 140 ml of the formulated mud into the viscometer plate, heating the mud to 120º F ± 2º F, rotating the viscometer at 100 RPM for 30 minutes, and extracting 10 mL of mud using a syringe with a cannula while recording the initial mud weight (m_1). Subsequently, the viscometer is halted, another 10 mL is extracted from the collection well, and its weight (m_2) is measured. The VSST (ppg) is then calculated using Eq. (3).

$$VSST = 0 \cdot 833(M_2 - M_1) \quad (3)$$

Vibrio fischeri was employed to evaluate the environmental impact of the formulated WBM in terms of toxicity. Being a rod-shaped gram-negative marine bacterium, Vibrio fischeri is commonly used for research on motility, biofilm formation, and bioluminescence due to its simplicity and non-pathogenic nature (Miyashiro et al., 2012). In our experiment, bacteria were cultured in photobacterium broth media, incubated at 24°C and 220 RPM in an incubator shaker for 24 hours. Bioluminescence, indicating toxicity, was observed using black 96-well plates. The bacteria were exposed to various drilling fluids, with purified water as a negative control and phenylarsine oxide (PAO) as a positive control at a final concentration of 330 µM.

Luminescence was measured using a coulter microplate reader at 490 nm after 60 minutes of exposure. Data were collected in triplicate, and the bioluminescence values were normalized with positive and negative controls to calculate relative toxicity. While the G50 Canadian rule stipulates that the bioluminescent value must exceed 75% after 15 minutes to meet toxicity criteria (Patel, 2009), our measurements extended the exposure time to 60 minutes to ensure prolonged interaction of the drilling fluid with the bioluminescent bacteria.

2.2 The Modeling Part

The modeling part in this study is based on coupling geomechanic with mud hydraulics. These assumptions for this model are the well is in an ideal borehole cleaning state; hence the effect of cuttings on the annular pressure is not considered, the Herschel Bulkley model is used to describe rheological drilling fluid, and the effect of pipe rotation is not considered. The geomechanic model will be built using TechLog software to determine minimum and maximum mud weight to drill ERW in the Permian basin.

The extension of open hole ERW must stop when the dynamic bottom hole pressure (P_{bh}) equals the fracture pressure (P_f) and this condition is represented as a critical point as seen in Fig.2. Mathematically, at this critical

point, the sum of hydrostatic pressure (P_{hy}) and annular pressure loss (ΔP_a) for all drilled sections is equal to the fracture formation pressure as demonstrated in Eqs (4)-7.

$$P_{bh} = P_f \quad (4)$$

$$P_{hy} + \Delta P_a = P_f \quad (5)$$

$$0 \cdot 052\rho_m L_v + \Delta P_a = 0 \cdot 052\rho_f L_v \quad (6)$$

$$0 \cdot 052\rho_m L_v + \left(\Delta P_v + \sum \Delta P_d + \Delta P_h\right) = 0 \cdot 052\rho_f L_v \quad (7)$$

Where, ρ_m is the drilling fluid density in ppg, L_v is the true vertical depth in ft, and ($\Delta P_v, \sum \Delta P_d, \Delta P_h$) are the pressure losses in psi which located in vertical, deviated, horizontal sections, respectively.

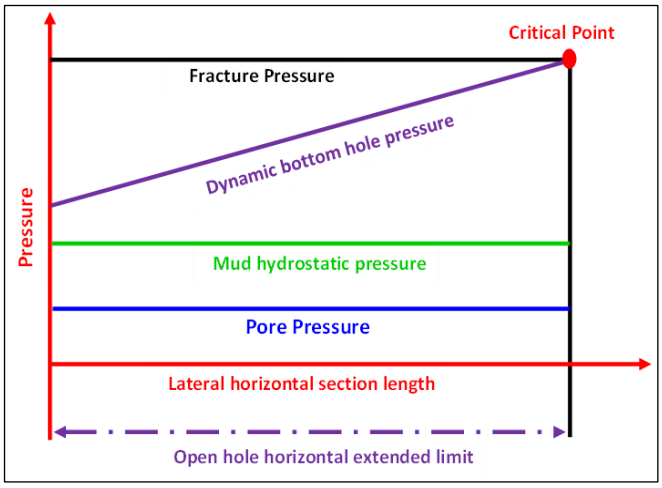

Fig. 2: Schematic of the horizontal-section limit (Metwally, 2024)

By rearranging Eq. (7), it is easy to calculate the maximum annular pressure loss in the open hole horizontal section using Eq. (8). Subsequently, once the pressure loss gradient in the horizontal section has been calculated, Equation (9) can be utilized to determine the limit for the open hole horizontal section (L_h) in Extended Reach Wells (ERW).

$$\Delta P_h = 0 \cdot 052(\rho_f - \rho_m)L_v - \left(\Delta P_v + \sum \Delta P_d\right) \quad (8)$$

$$L_h = \frac{\Delta P_h}{(\Delta P/\Delta L)_h} \quad (9)$$

2.2.1 Pressure Loss Calculations Based on Herschel Buckley Rheological Model

The Herschel–Bulkley model outperforms the Bingham plastic and power law rheological models in predicting and accurately simulating drilling fluid rheology (Folayan et al., 2016). Consequently, the Herschel–Bulkley model is employed for calculating annular pressure loss. The shear stress (τ_y) is determined at a shear rate of 0.1 S^{-1} using the OFITE 900 viscometer. The Herschel–Bulkley model parameters (n and k) will be computed through regression analysis, as outlined in Equations (11) and (12).

$$\tau = \tau_y + K\gamma^n \quad (10)$$

Where: τ_y is yield stress (lbf/100 ft^2), n is flow behavior index, K is Flow consistency index ((lbf. S^n/100 ft^2), τ is shear stress (lbf/100 ft^2), and γ is the shear rate (S^{-1})

$$n = \frac{\sum \log(\tau - \tau_y) \sum \log(\gamma) - N \sum (\log(\tau - \tau_y) \log(\gamma))}{(\sum \log \gamma)^2 - N \sum (\log \gamma)^2} \quad (11)$$

$$\log(K) = \frac{\sum \log(\tau - \tau_y) - n \sum \log(\gamma)}{N} \quad (12)$$

The calculations of annular pressure loss are contingent on the flow regime, whether it is laminar or turbulent. The determination of the flow regime utilizes the Reynolds number (N_{Re}) and critical Reynolds number (N_{Rec}), employing the Herschel–Bulkley model, as illustrated in Equations (14) and (16) (Guo and Liu, 2011).

$$v = \frac{q}{2{\cdot}448(d_o^2 - d_i^2)} \quad (13)$$

Where: v is the average fluid velocity in the annulus, q is pump flow rate in gpm, and d is diameter in inch. The subscripts i and o are for inner and outer, respectively.

$$N_{Re} = \frac{4(2n+1)}{n}\left[\frac{\rho v^{(2-n)}\left(\frac{d_o - d_i}{2}\right)^n}{\tau_y\left(\frac{d_o - d_i}{2v}\right)^n + K\left(\frac{2(2+1)}{nC_a^*}\right)^n}\right] \quad (14)$$

$$C_a^* = 1 - \left(\frac{1}{n+1}\right)\frac{\tau_y}{\tau_y + K\left\{\frac{2q\,(2n+1)}{n\pi\left[\frac{d_o}{2} - \frac{d_i}{2}\right] * \left[\left(\frac{d_o}{2}\right)^2 - \left(\frac{d_i}{2}\right)^2\right]}\right\}^n} \quad (15)$$

$$N_{Rec} = \left[\frac{8(2n+1)}{ny}\right]^{\frac{1}{1-z}} \quad (16)$$

$$y = \frac{\log(n) + 3 \cdot 93}{50} \quad (17)$$

$$z = \frac{1 \cdot 75 - \log(n)}{7} \quad (18)$$

Equations 14 and 15 express the flow rate (q) in ft^3/s, the d_i and d_0 are in ft, and the fluid density (ρ) is in lb/ft^3.

If $N_{Re} < N_{Rec}$, then the flow is laminar, and the annular pressure loss gradient is calculated using Eq. (19).

$$\frac{\Delta P}{\Delta L} = \frac{4K}{14400(d_o - d_i)}\left\{\left(\frac{\tau_y}{K}\right) + \left[\left(\frac{16(2n+1)}{nC_a^*(d_o - d_i)}\right)\left(\frac{q}{\pi(d_o^2 - d_i^2)}\right)\right]^n\right\} \quad (19)$$

If $N_{Re} > N_{Rec}$, the flow is turbulent, and the annular pressure loss gradient is calculated using Eq. (20).

$$\frac{\Delta P}{\Delta L} = \frac{f_a\, q^2\, \rho_m}{1421 \cdot 22(d_o - d_i)\left(d_o^2 - d_i^2\right)^2} \quad (20)$$

$$f_a = y(C_a^* * N_{Re})^{-z} \quad (21)$$

Therefore, the annular pressure drop using concentric drill pipe inside the well can be expressed using the following equation 22, and 23.

If the flow is laminar

$$\Delta P = \frac{4K}{14400(d_o - d_i)}\left\{\left(\frac{\tau_y}{K}\right) + \left[\left(\frac{16(2n+1)}{nC_a^*\,(d_o - d_i)}\right)\left(\frac{q}{\pi\left(d_o^2 - d_i^2\right)}\right)\right]^n\right\}\Delta L \quad (22)$$

If the flow is Turbulent

$$\Delta P = \frac{f_a\, q^2\, \rho_m}{1421 \cdot 22(d_o - d_i)\left(d_o^2 - d_i^2\right)^2}\Delta L \quad (23)$$

2.2.2 Procedures to Calculate Open Hole Horizontal Extension Limit

The calculation procedures of the modified geomechanics hydraulic model are summarized as following:

(1) Calculate the fracture pressure p_f using Techlog geomechanic Analysis software.
(2) Calculate the annular pressure drops ΔP_V, ΔP_{ds}, and ΔP_{dl} of the vertical section, small-inclination section, and long deviation inclination respectively, using Eq. (22) or (23);
(3) Calculate the pressure loss gradients in the horizontal section $(\Delta p/\Delta L)_h$ using Eq. (19) or (20);
(4) Calculate maximum hydraulic friction loss in open hole horizontal section in ERW using Eq. (8)
(5) Calculate the open hole horizontal-section limit l_h using Eq. (9).

3. RESULTS AND DISCUSSIONS

The basic WBM in this study was composed of bentonite, caustic soda to adjust pH, starch, and PAC-L to reduce fluid loss, XC polymer to provide viscosity, and KCl salt to stabilize shale, and Barite to control mud density. The additives of basic WBM with its concentration were tabulated in table 1. But the main additive to develop high performance WBM is emulsified anionic polyacrylamide FR. The main function groups in FR are the amide group ($CONH_2$), carboxylic groups (COOH), and carboxylate group (COO^-). In the basic medium, carboxylic group (COOH) is ionized to negative carboxylate group COO^-.

The developed WBM is the fluid that contain FR with the main additives like bentonite, caustic soda, starch, PAC-L, XC polymer, KCl, and barite and were mentioned also in table 1. The initial phase of this investigation involves experimental assessments of the developed WBM, focusing on rheological stability and shale inhibition. To gauge the thermal stability of the formulated WBM, mud rheology will be measured at various temperatures representative of Wolfcamp and Spraberry formations' conditions using the OFITE 900 viscometer.

Table 1: Mud additives for both basic and developed WBM

	WBM without FR		WBM with FR	
	pH (8.5-9.5)		pH (8.5-9.5)	
Additives	Quantities	Unit	Quantities	Unit
Water	1	bbl	1	bbl
Bentonite	8	lb/bbl	8	lb/bbl
NaOH	0.5	lb/bbl	0.5	lb/bbl
FR	0	lb/bbl	0.5	lb/bbl
Starch	3	lb/bbl	3	lb/bbl
PAC-L	1	lb/bbl	1	lb/bbl
XC polymer	0.75	lb/bbl	0.75	lb/bbl
KCl	17.5	lb/bbl	17.5	lb/bbl
Barite	As required	lb/bbl	As required	lb/bbl

The mud rheology investigates the shear stress of WBM samples under varying shear rates at temperatures of 120°F, 150°F, and 180°F, as presented in Table 1 and graphically depicted in Fig.3, and Fig.4. The data in Fig.4 reveals that the fluid rheology of WBM without FR experienced thermal degradation, evident by a decrease in measured shear stress as the temperature rose from 120°F to 180°F. Conversely, WBM with 0.5 lb/bbl FR concentration exhibited higher thermal stability than its FR-absent counterpart, as evidenced in Fig.3. This enhanced stability arises from the interaction between FR and bentonite.

The electrostatic attraction between the negative carboxylate group (COO^-) and the positive bentonite edge, coupled with the formation of hydrogen bonds between the amide group on the FR surface and the hydroxide groups on the bentonite's negative surface, facilitates this interaction. The strength of these hydrogen bonds increases with rising temperatures (Mpofu et al., 2004). Additionally, the presence of KCl salt acts as a bridging agent between the negative groups on the FR surface and the negative bentonite, reinforcing the attractive forces between FR and bentonite. Consequently, these interactions contribute to the stability in rheology as the temperature escalates from 120°F to 180°F.

Moreover, the formulated WBM with FR demonstrates enhanced low-end rheology in comparison to FR-free WBM. A heightened low-end rheology, reflecting increased apparent viscosity at low shear rates, plays a crucial role in efficiently transporting drilling cuttings and suspending weighting materials (Ghanbari et al., 2015). This underscores the improved suspension capabilities of the formulated WBM for drilling cuttings in contrast to WBM lacking FR. Besides, high low-end rheology will improve suspending weighting material and prevent sagging problem during drilling operation.

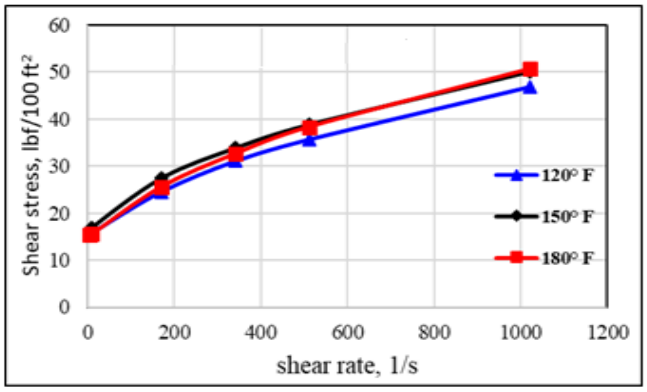

Fig. 3: Shear stress versus shear rate for the formulated WBM with 0.50 lb/bbl FR

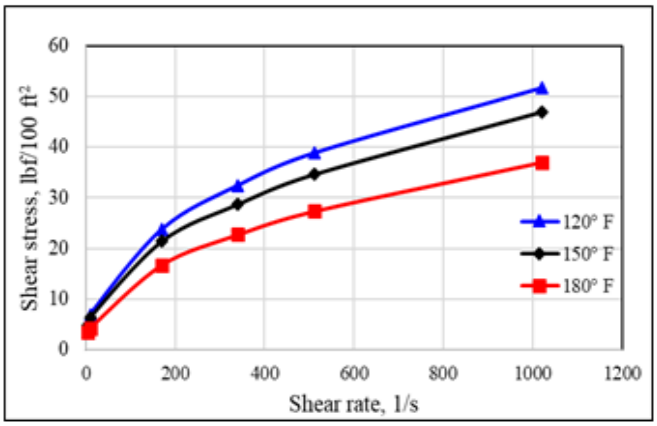

Fig. 4: Shear stress versus shear rate for the formulated WBM without FR

Clearly, the addition of FR improves the fluid rheology of WBM and enhances its thermal stability. The current focus is on assessing the effectiveness of the developed WBM with FR for shale inhibition. This assessment involves shale dispersion test, accretion bit balling test and contact angle analysis.

Shale dispersion tests were conducted to determine the percentage of shale recovery when using a formulated WBM containing 0.25 and 0.50 lb/bbl of FR. The shale cuttings used in the experiment were obtained from the Wolfcamp shaly formation. The results of the shale recovery from the dispersion tests are presented in Table 2. With FR concentrations of 0.25 and 0.50 lb/bbl, shale recovery reached 90% and 98%, respectively, compared to 60% for WBM without FR. This suggests that FR effectively inhibits shale dispersion by preventing water-shale interaction.

Table 2: Shale dispersion test results for WBM with and without AFR

Mud Type	Shale Recovery (%)
WBM with 0.00 lb/bbl FR	60
WBM with 0.25 lb/bbl FR	90
WBM with 0.50 lb/bbl FR	98

The electrostatic attraction between negative carboxylate groups and positive clay edges, as well as the formation of hydrogen bonds between the amid group on FR and the negative clay surface, contribute to these inhibitory effects. These interactions, coupled with the high molecular weight of FR, enable it to encapsulate the shale or clay surface and prevent water-shale interaction. Consequently, the formulated WBM containing FR demonstrates the capability to inhibit shale swelling and dispersion.

The following test for evaluation shale inhibition performance for the developed WBM is anti-accretion bit balling test. Bit balling occurs when drill cuttings adhere to the bit surface while drilling through gumpo clays, water-reactive clays, and shale formations. This phenomenon can cause several issues, such as a decrease in the rate of penetration, increased surface torque, and elevated standpipe pressure (Stefano et al., 2009). Resolving bit balling may involve pulling the bottom hole assembly out of the hole to address the balling problem at the bit.

In this research, bentonite tablets with a high Cation Exchange Capacity (CEC) of 40 meq/100 gm were utilized, indicating their significant swelling capability. Accretion tests were conducted with varying clay weights (25, 50, 75, and 100 gm) added to different WBM formulations. Fig. 5 illustrates the clay accretion profile after immersion in WBM without KCl and FR. The results demonstrate a noticeable increase in clay sticking with the addition of clay tablets, leading to shale accretion that can result in bit balling and a reduction in the rate of penetration.

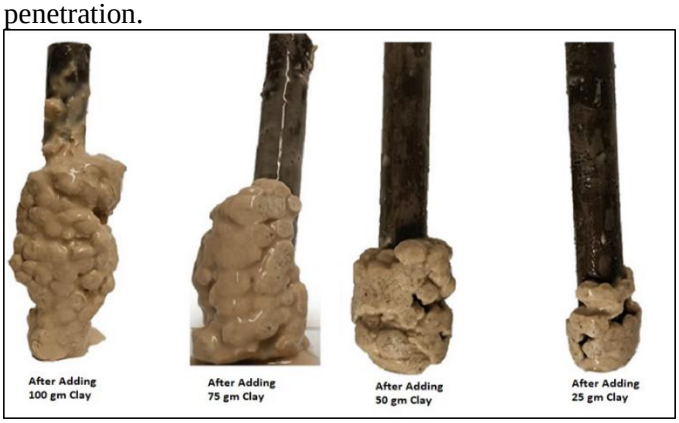

Fig. 5: Clay accretion profile in the basic WBM

Conversely, the introduction of FR into the formulated WBM containing KCl effectively prevented shale accretion on the steel bar, even with an increased shale amount ranging from 25 gm to 100 gm, as illustrated in Fig. 6. Consequently, the formulated WBM with FR showcased the ability to avert shale sticking and bit balling while simultaneously improving the Rate of Penetration.

The key to FR's ability to prevent bit balling lies in its manufacturing process as an emulsified copolymer synthesized in the presence of a surfactant. This surfactant forms a barrier between the clay surface and the solid bar, inhibiting sticking. As a result, the accretion percentage of shale in WBM with AFR remained below 1% (Fig. 7), indicating that AFR not only hinders shale swelling and dispersion but also effectively prevents shale accretion, thereby minimizing the bit balling issue.

Fig. 6: Clay accretion profile in WBM with FR

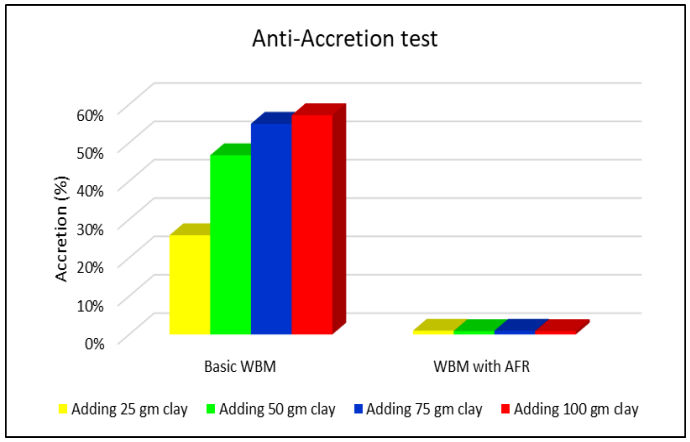

Fig. 7: Accretion percentage of the formulated WBM with and without AFR

The third examination employed for assessing the suitability of the developed WBM with FR as a shale inhibitor involves the measurement of the contact angle. Normally, the contact angle is influenced by the wettability of the clay surface. Fig.8 depicts the contact angle between a water droplet and the shale surface after immersion in basic WBM. The observed contact angle is approximately 12.1°, indicating that the shale surface is hydrophilic and inclined to adsorb water. Conversely, the addition of 0.5 lb/bbl FR to WBM results in an increase in the contact angle from 12.1° to 50.7°, as shown in Fig. 9. This suggests a change in shale surface wettability, transitioning from being more hydrophilic to becoming less hydrophilic and more hydrophobic. when the shale surface exhibits increased hydrophilicity, it will resist water absorption, leading to the prevention of swelling and dispersion in shale.

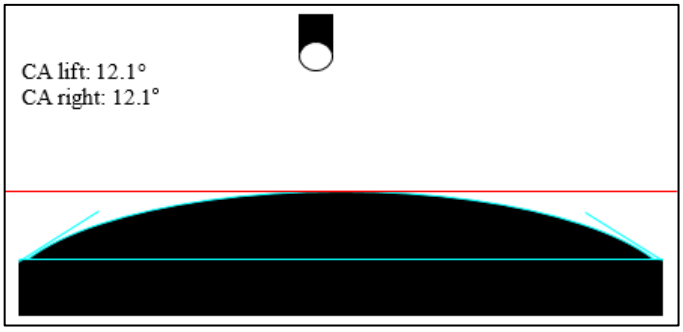

Fig. 8: Contact angle measurements of basis WBM

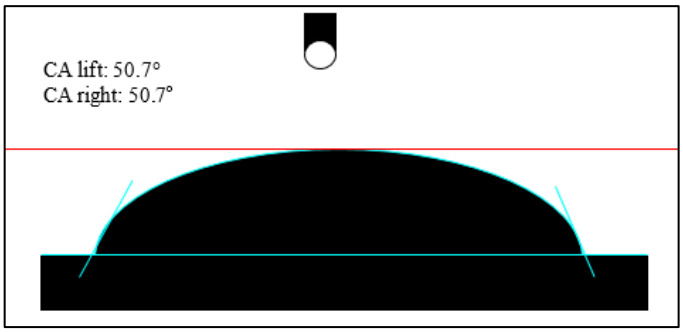

Fig. 9: Contact angle measurements of WBM with FR

The developed WBM with FR had the ability to inhibit shale, mitigate bit balling problem, and alter shale wettability surface. There is an additional required test to evaluate performance of developed WBM in terms of barite sagging. As barite sagging is acritical challenging in drilling ERW operation. Barite sagging refers to the separation of barite (weighting material) from the liquid phase, causing it to settle down. This phenomenon can lead to variations in mud density, posing an increased risk of kicks or well control problems (Mohamed et al., 2020). This can also limit ERW extension.

To address this issue, it is crucial for the drilling mud to exhibit favorable rheological properties that mitigate barite sagging. The formulated WBM, both with and without FR, underwent testing VSST to assess their sag tendency. The VSST test procedures were outlined in the experimental apparatus section. WBMs with different densities ranging from 9 to 13 ppg were prepared, and VSST values were calculated using Eq. 3. A VSST value below 1 ppg indicates minimal sagging tendency, while a value exceeding 1.6 ppg suggests the possibility of sag problems (Bern et al., 2010). A drilling fluid with a VSST less than 1 ppg is considered effective for suspending weighting material with minimal risk of sagging.

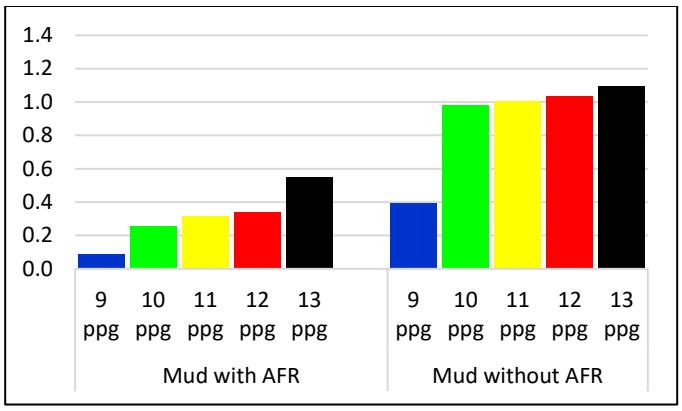

Fig.10: VSST of the formulated WBM measured at 100 RPM.

The results of the VSST, presented in Fig. 10, reveal that the WBM with FR exhibits lower VSST values compared to the WBM without AFR across all mud densities ranging from 9 to 13 ppg. The VSST of WBM without FR is at least twice the value observed for WBM with FR.

An effective WBM, especially in the absence of circulation, requires a supportive gel structure to suspend barite and prevent sagging. The interaction between FR and bentonite, in the presence of the electrolyte formed, enhances this gel structure. Consequently, the developed WBM with FR demonstrates the ability to suspend barite-weighting material and minimize sagging problems.

The preceding outcomes illustrate the efficiency of the formulated WBM with FR in addressing barite sagging, suppressing shale, averting bit balling issues, and thermally stabilizing mud rheology up to 180°F. To be employed in drilling operations, the drilling fluid must meet performance standards and comply with environmental regulations. As previously mentioned, the developed WBM with FR meets the necessary performance criteria, and the remaining aspect to be examined is its environmental compatibility. This study conducted toxicity tests to assess the impact of the formulated WBM with FR on bioluminescence, providing insights into its environmental ramifications. To meet the G50 Canadian standards for toxicity, the living bioluminescence percentage after 15 minutes must exceed 75%. This study extended the exposure time to different WBM up to 60 minutes to better understand their impact on bacteria life.

The measurements of living bioluminescence are detailed in Fig. 11. With an FR concentration of 0.50 lb/bbl, both WBM with and without FR exhibited bioluminescence percentages surpassing 75%. Even when the formulated WBMs were diluted tenfold, the bioluminescence value remained above 75%. Therefore, the formulated WBM containing FR is recognized as an environmentally friendly drilling fluid with minimal impact on the ecosystem, as indicated by the toxicity measurements.

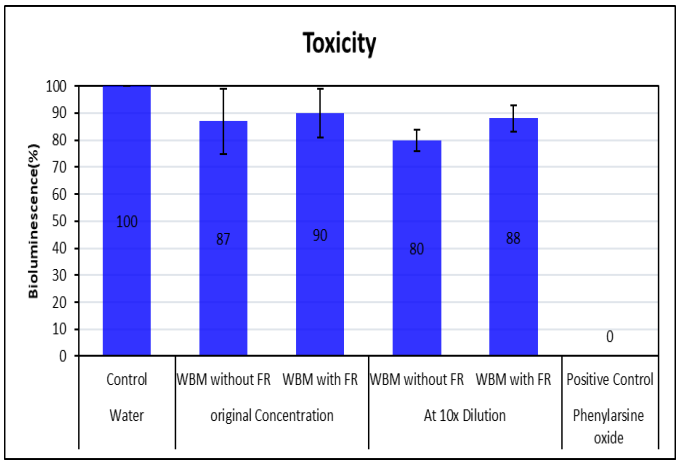

Fig.11: The bioluminescence assessments for the formulated WBM with/ without FR

The next phase involves the theoretical application of the environmentally friendly WBM with FR for drilling ERW within the Permian Basin, specifically targeting the Wolfcamp and Spraberry formations. The objective is to assess the potential increase in the horizontal extension limit of the drilling open hole, utilizing both mud hydraulics and geomechanics, as illustrated in the modeling section. Geomechanics analysis is a systematic approach that plays a pivotal role in both assessing the mechanical behavior of rocks around a wellbore and in the prediction of pore pressure and fracture pressure. It involves integrating geological, geophysical, and engineering data to develop predictive models that not only anticipate potential instabilities but also guide drilling operations effectively to predict open hole horizontal extension. The key parameters considered in geomechanics analysis for wellbore stability and pressure predictions encompass in-situ stress conditions, rock compressive strength, rock tensile strength, pore pressure, and the effects of drilling fluid circulation.

The geomechanical analysis utilized Techlog software, with input logs comprising density, gamma ray, neutron, compression, and shear sonic logs. The initial phase involved the computation of in situ stresses, including vertical overburden stress (rb_SigV), maximum horizontal stress (rb_TYSP), and minimum horizontal stress (rb_TXSP). The findings reveal a normal fault regime in the Midland Basin, evidenced by the order of vertical stress > maximum horizontal stress > minimum horizontal stress, as illustrated in Fig. 12. Besides, the values of minimum and maximum horizontal stresses is calibrated based on the calculated Fracture pressure by adjusting the value for maximum principal horizontal strain in Techlog software. Additionally, the uniaxial compressive strength (rb_UCS) and tensile strength (rb_TSTR) were determined and presented in Fig. 12.

The following step is to determine pore pressure (PP) and Fracture pressure (FP). The calculated equivalent density for fracture pressure and pore pressure were calculated

and shown in Fig. 13. The precision of forecasted fracture pressure hinges on its alignment with the fracture pressure derived from the Diagnostic Fracture Injection Test (DFIT). As depicted in Figure 13, there is a strong correspondence between the predicted fracture pressure and the available DFIT data, showcasing the accuracy of fracture pressure prediction through the utilization of geomechanical analysis in this study. The accurate prediction of FP and PP is Pivotal to determine optimum mud weight window for better wellbore stability.

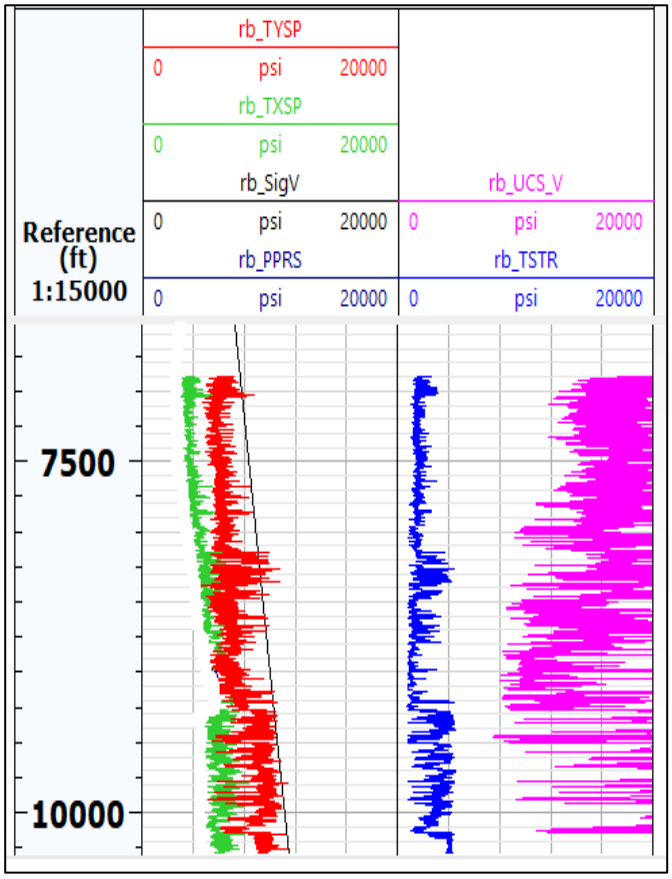

Fig. 12. The calculated principal stresses, unconfined compression strength, and tensile strength for drilled formations in the midland basin

Identifying the orientation of maximum and minimum horizontal stresses is a crucial step in optimizing the well path and conducting stability analyses for the wellbore. The minimum horizontal direction especially in midland basin is parallel to North-South direction (Snee et al, 2018). The horizontal wells in the Permian basin were drilled in the direction parallel to minimum horizontal stress and perpendicular to maximum horizontal stress. Fig. 14 depicts a schematic representation of the horizontal well drilled in the Permian Basin, aligned parallel to the minimum horizontal stress. The 8.5-inch hole was drilled in the Spraberry shale formation, and the drilling parameters for this well are presented in Table 3

Table 3: Parameters list for the drilled horizontal well

Input parameters	Value	Unit
Outside diameter of drill pipe	5	Inch
Inside diameter of casing	8.88	Inch
True Vertical Depth (TVD)	9020	ft
Kick off Point (KOP)	8233	ft
Flow Rate	846	gpm
ECD at 12600 ft (measured depth)	9.17	ppg
Rate of Penetration	185	ft/hr

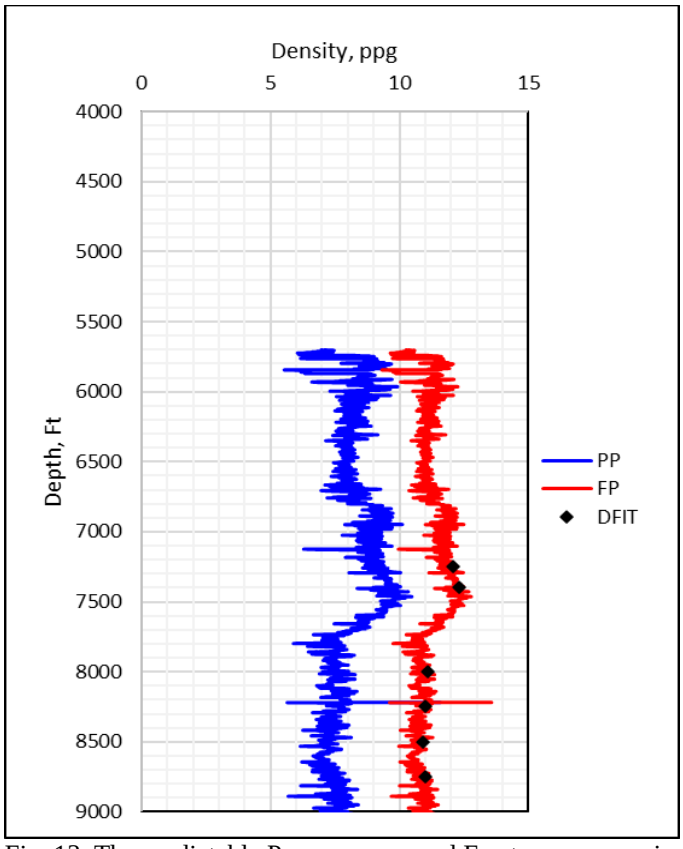

Fig. 13. The predictable Pore pressure and Fracture pressure in the midland basin

The geomechanic study is powerful tool to efficiently determine minimum and maximum mud weight (operating mud weight window) to drill the sketch horizontal well. To prevent break down, the geomechanics study verified the mud weight should be less than 10.6 ppg (Fig. 15). In addition, the used mud weight should be higher than 8.5 to prevent shear failure (Fig. 16). Hence, the Sensitivity analysis shows the optimum mud weight is range from 8.5 to 10.6 ppg to drill horizontal well parallel to minimum horizontal stress in Spraberry formation in the midland basin (Fig. 17).

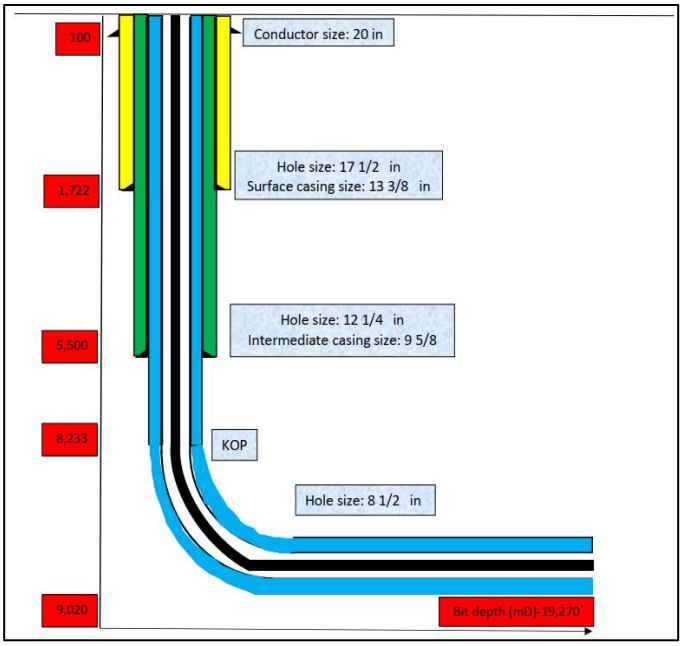

Fig. 14: Wellbore sketch in Spraberry formation with casing sizes

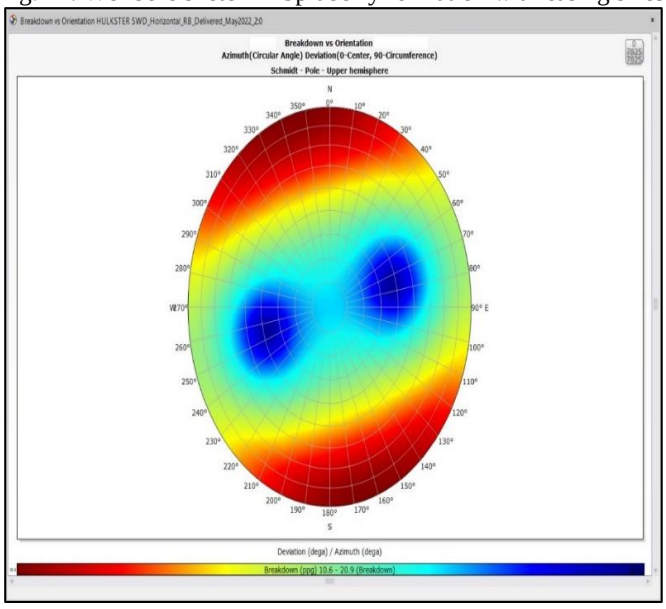

Fig. 15: Breakdown density vs well Orientation

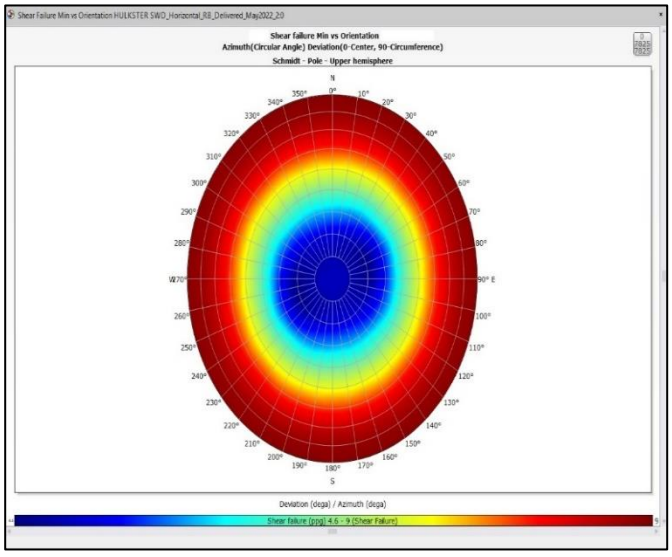

Fig. 16: Shear Failure density vs well Orientation

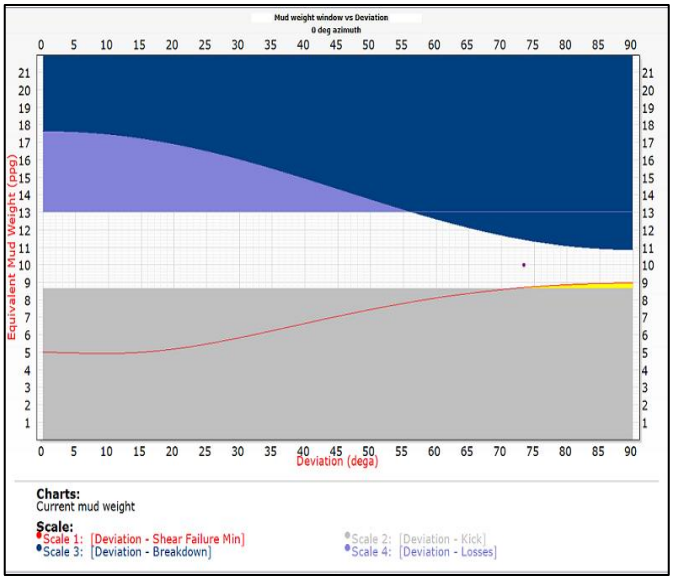

Fig. 17: Sensitivity analysis of equivalent mud weight versus well deviation

The hole of 8.5 inch was drilling in Spraberry shale formation using OBM and its properties was measures at 120° F and mentioned in Table 4. In addition, the circulation rate in 8.5 inch hole was 846 gallon per minute. The Hershel-Buckley model parameters (τ_y, K and n) at 120° F were calculated using regression analysis as seen in table 4. The calculated R^2 demonstrates the accuracy of the calculated Hershel-Buckley model parameters to predict mud rheology in comparison with the measured mud rheology. All R^2 values are higher than 0.98. Therefore, the high accuracy of the calculated Hershel-Buckley model parameters will lead to efficient prediction of open hole extended horizontal section. In this study, the extension of open hole horizontal section is limited when bottom hole dynamic pressure reaches fracture pressure.

Table 4: The Calculated value of Hershel-Buckley parameters for different formulated muds

	WBM without FR	WBM with FR	OBM
Shear stress at 600 RPM, DR	16	29	34
Shear stress at 300 RPM, DR	11	20	22
Shear stress at 200 RPM, DR	9	17	19
Shear stress at 100 RPM, DR	7	13	13
Shear stress at 6 RPM, DR	6	8	9
Shear stress at 3 RPM, DR	5	7	7
τy (lbf/100 ft^2)	5.3	7.24	7.96
n	0.94	0.77	0.88
K (lbf.S^n/100 ft^2)	0.016	0.11	0.06
R^2	0.986	0.998	0.996

To verify the precision of the hydraulic model using the Hershel-Buckley model for calculating annular pressure loss, the calculated Equivalent Circulation Density (ECD) was compared to the measured ECD at a measured depth

MD of 12600 ft, as detailed in table 3. The calculated ECD, established on a mud density of 8.75 ppg, at MD 12600 ft was 9.16 ppg, while the measured ECD was 9.17 ppg at the same depth. Consequently, the difference between the calculated and measured ECD is approximately 0.1%, highlighting the model's high accuracy in ECD computation. Given the Hershel-Buckley model's accuracy in assessing annular pressure losses and ECD, the subsequent step involves determining the open hole horizontal extension limit.

The maximum extension limit of an open hole is influenced by various factors, including mud density, mud type, and the operating circulation rate. Fig. 18 illustrates how the mud density of different mud types affects the horizontal section limit at a circulation rate of 846 gpm. This specific rate was the actual pumping rate employed during the drilling of an 8.5-inch hole section.
Generally, the open hole horizontal section limit tends to decrease as mud weight increases. A comparison reveals that the limit for drilling open hole horizontal sections with both OBM and WBM with FR is higher than that of formulated WBM without FR. It is visually observed that drilling open hole horizontal sections using WBM without FR becomes impractical when mud density reaches 10 ppg.
The maximum horizontal section length achievable with WBM formulated without FR is approximately 8,800 ft, given a density of 8.75 ppg at a circulation rate of 846 gpm. However, when FR is added to WBM with a density of 8.75 ppg at the same circulation rate, the maximum horizontal length increases to 12,500 ft. This surpasses the 11,900 ft horizontal section drilled with OBM at the same density and circulation rate.
On the contrary, if the circulation rate decreases to 700 gpm, there won't be a significant difference in the horizontal section length limit between drilling with OBM and formulated WBM with FR, as depicted in Fig. 19. Additionally, Fig. 19 clearly indicates that a decrease in circulation rate from 846 gpm to 700 gpm results in a rapid increase in the open hole horizontal section limit, particularly when using OBM and WBM with FR.

Conversely, when the circulation rate is increased to 1000 gpm, the use of formulated WBM with FR is recommended for drilling open hole horizontal sections, as illustrated in Fig. 20. The calculated limits for drilled open hole horizontal sections at 8.75 ppg and 1000 gpm were 9300 ft and 4500 ft for WBM with FR and OBM, respectively. This suggests that the developed WBM with FR is advisable for high circulation rates because FR has the capability to reduce hydraulic friction losses. Consequently, this extension in the horizontal section limit contributes to increased hydrocarbon production.

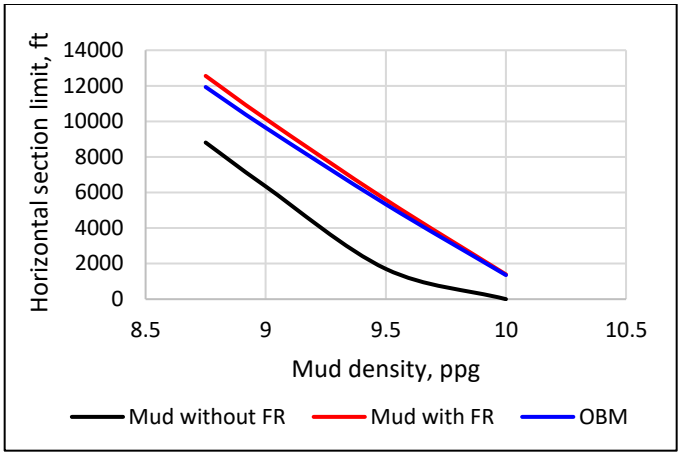

Fig. 18: Open hole horizontal extension limit at flow rate of 846 gpm

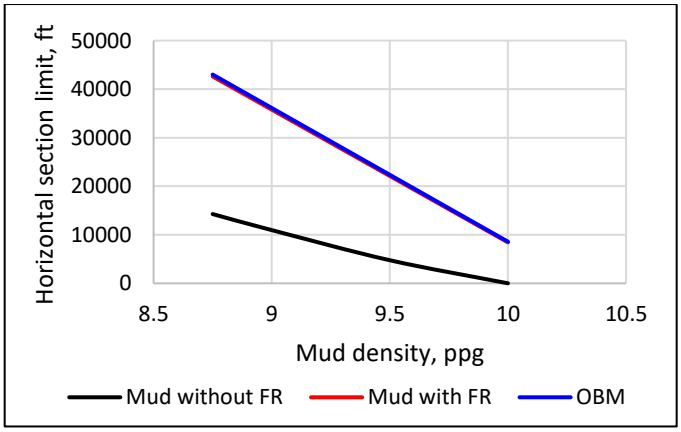

Fig. 19: Open hole horizontal extension limit at flow rate of 700 gpm

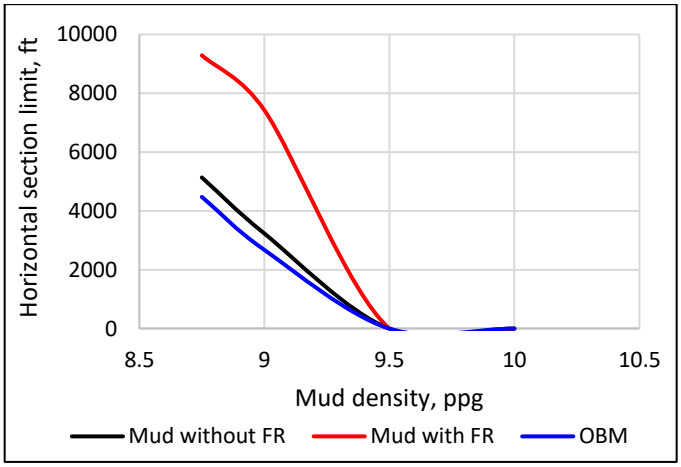

Fig. 20: Open hole horizontal extension limit at flow rate of 1000 gpm

It became evident that the addition of FR to WBM effectively reduces hydraulic frictional pressure loss, particularly in turbulent flow. This reduction contributes to a decrease in equivalent circulation density during drilling. The formulated WBM with FR will be recommended for drilling wells, especially in narrow windows between pore pressure and fracture pressure.

Additionally, a sensitivity analysis was conducted to determine the increase in drilling open hole horizontal section when transitioning from using OBM to the developed WBM with FR. According to Fig. 21, the developed WBM with FR did not provide added value at a circulation rate of 700 gpm. However, as the pumping rate increased from 700 gpm to 864 gpm and 1000 gpm, the impact of FR in WBM became obvious, aiding in the extension of open hole horizontal section. The use of WBM with 0.5 lb/bbl FR instead of OBM resulted in a significant 5000 ft increase in drilling horizontal section. This elongation is poised to maximize reservoir contact and enhance hydrocarbon production.

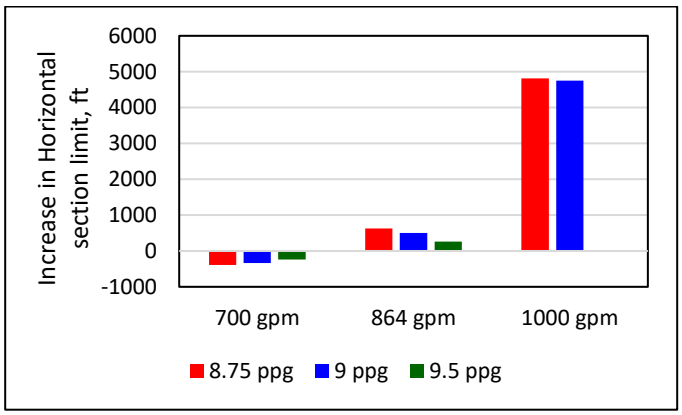

Fig. 21: Amount of increase in horizontal section limit by using the developed WBM in comparison with OBM.

4. CONCLUSION

This paper presents experimental research on formulating environmentally friendly high-performance WBM using FR. The focus is on developing a WBM with FR to address various challenges in the Permian Basin, including inhibiting shale problems, resisting thermal degradation, mitigating barite sagging, ensuring environmental friendliness with minimal impact on the ecosystem, and approaching OBM performance. The study includes geomechanics analysis to determine the operating mud weight window. Additionally, the geomechanic analysis is coupled with the Hershel-Buckley hydraulic model to assess the increase in open hole extensional limit of horizontally drilled wells using the formulated OBM and the developed WBM with FR. The key conclusions drawn from the study are as follows:

- The formulated WBM with FR effectively resists thermal mud degradation up to 180°F.
- Shale dispersion and Accretion tests demonstrate the efficiency of the developed WBM with FR in inhibiting shale and preventing bit balling problems.
- Contact angle measurements indicate that FR changes the shale surface wettability from hydrophilic to hydrophobic.
- The developed WBM with FR shows low impact on the ecosystem and is environmentally friendly, as confirmed by bioluminescence measurements.
- The developed WBM with FR suspended weighting material and mitigate barite sagging.
- The safe mud weight window to drill horizontal well in the Spraberry formation in the Midland basin is range from 8.5 to 10.6 ppg.
- The hydro-geomechanical model predicts open hole concentric Effective Rigidity of Wellbore (ERW) limits at 12,500 and 10,000 feet when using the developed WBM with densities of 8.75 and 9.0 ppg, respectively, at a circulation rate of 864 gpm.
- The developed WBM with FR is recommended over OBM especially at high circulation rates.
- The formulated WBM with FR could be a viable replacement for OBM when drilling long ERW lateral sections in the Permian basin.

Nomenclature

P_{bh}	Bottom hole pressure, psi
P_f	Fracture pressure, psi
P_{hy}	Mud hydrostatic pressure, psi
ΔP_v	Annular pressure drop of vertical section, psi
ΔP_d	Annular pressure drop of deviated section, psi
ΔP_h	Annular pressure drop of horizontal section, psi
ρ_f	The equivalent density of the fracture pressure, ppg
ρ_m	Mud density, ppg
L_v	The vertical section length, ft
L_h	The horizontal section limit, ft
v	Average annular velocity, ft/s
q	Mud flow rate
MD	Measured Depth, ft
d_o	The casing inner diameter or wellbore diameter
d_i	The drill pipe outer diameter, inch
$\frac{\Delta P}{\Delta L}$	Pressure loss gradient, psi/ft
f_a	The annular friction factor
Pp	Pore pressure
Fp	Fracture pressure
Lbf	Pound Force
ppg	Pound Per Gallon
DR	Dial reading
KOP	Kick off point
XC	Xanthan Gum polymer
PAC	Polyanionic cellulose
Lb/bbl	Pound per barrel
KCl	Potassium Chloride salt
WBM	Water based mud
OBM	Oil based mud
ECD	Equivalent circulation density, ppg
µM	MicroMeter
µL	Microliter

Conversions

Lbf/100 ft^2 = 1.07 x DR
1/S = 1.703 x RPM

REFERENCES

1. Aften C., Watson, W. (2009). Improved Friction Reducer for Hydraulic Fracturing, Presented at the SPE Hydraulic Fracturing Technology Conference in Woodlands, TX. SPE-118747-MS. https://doi.org/10.2118/118747-ms
2. Ahmed, H. M., Kamal, M. S., & Al-Harthi, M. (2019). Polymeric and low molecular weight shale inhibitors: A review. Fuel, 251, 187–217. https://doi.org/10.1016/j.fuel.2019.04.038
3. Ashena, R., Hekmatinia, A., Ghalambor, A., Aadnøy, B. S., Enget, C., & Rasouli, V. (2021). Improving drilling hydraulics estimations-a case study. Journal of Petroleum Exploration and Production Technology, 11(6), 2763–2776. https://doi.org/10.1007/s13202-021-01203-4
4. Abdulaziz, A. M., Metwally, M., & Dahab, A. S. (2018). Petrophysical analysis and flow units characterization for Abu Madi pay zones in the Nile Delta reservoirs. Open Journal of Geology, 08(12), 1146–1165. https://doi.org/10.4236/ojg.2018.812070
5. Bagheri, H., Tanha, A. A., Ardejani, F. D., Heydari-Tajareh, M., & Larki, E. (2021). Geomechanical model and wellbore stability analysis utilizing acoustic impedance and reflection coefficient in a carbonate reservoir. *Journal of Petroleum Exploration and Production Technology*, *11*(11), 3935–3961. https://doi.org/10.1007/s13202-021-01291-2
6. Bern, P.A.; Zamora, M.; Hemphill, A.T.; Marshall, D.; Omland, T.H.; Morton, E. (2010). Field Monitoring of Weight-Material Sag. In Proceedings of the 2010 AADE Fluids Conference and Exhibition, Houston, TX, USA.
7. Bradshaw, P. (1974). Possible origin of Prandtl's mixing-length theory. Nature, 249(5453), 135–136. https://doi.org/10.1038/249135b0
8. Chamat, E. H., Cuadros, G., Trejo, E. D., Scrofina, J., Cermeno, E., & Rodríguez, O. A. (2015). Performance step change in shallow extended reach wells in Venezuela enables drilling optimization and increased heavy oil production. All Days. https://doi.org/10.2118/174443-ms
9. Chen, X., & Gao, D. (2017). The Maximum-Allowable well depth while performing Ultra-Extended-Reach drilling from shallow water to deepwater target. Spe Journal, 23(01), 224–236. https://doi.org/10.2118/183025-pa
10. Folayan JA, Anawe PAL, Abioye PO, Elehinafe, FB. Selecting the Most Appropriate Model for Rheological Characterization of Synthetic Based Drilling Mud. Inter J App Eng Res. 2016;12(18)7614-7629
11. Gyimah, E., Metwally, M., Tomomewo, O. S., Hurtado, J. P., Alamooti, M., and W. Gosnold. (2023). Geothermal Energy Storage: A Conceptual Assessment of Geologic Thermal Storage Systems in North Dakota. Paper presented at the 57th U.S. Rock Mechanics/Geomechanics Symposium, Atlanta, Georgia, USA. doi: https://doi.org/10.56952/ARMA-2023-0390
12. Ghanbari S, Kazemzadeh E, Soleymani M, Naderifar, A. A facile method for synthesis and dispersion of silica nanoparticles in water-based drilling fluid. Colloid Poly Sci. 2015;294(2):381-388.
13. Guo B, Liu G. Applied Drilling Circulation Systems: hydraulics, calculations, and models. 2011. https://doi.org/10.1190/tle37020127.1
14. Ishak, K. E. H. K., Khan, J. A., Padmanabhan, E., & Ramalan, N. H. M. (2023). Friction reducers in hydraulic fracturing fluid systems – A review. AIP Conference Proceedings. https://doi.org/10.1063/5.0114174
15. Jain, R., Mahto, V., & Sharma, V. (2015). Evaluation of polyacrylamide-grafted-polyethylene glycol/silica nanocomposite as potential additive in water based drilling mud for reactive shale formation. Journal of Natural Gas Science and Engineering, 26, 526–537.
16. Khaled, S., Soliman, A. A., Mohamed, A., Gomaa, S., & Attia, A. (2022). New Models for Predicting Pore Pressure and Fracture Pressure while Drilling in Mixed Lithologies Using Artificial Neural Networks. ACS Omega, 7(36), 31691–31699. https://doi.org/10.1021/acsomega.2c01602
17. Li, J., Zhou, X., Gayubov, A., & Shamil, S. (2023). Study on production performance characteristics of horizontal wells in low permeability and tight oil reservoirs. Energy, 284, 129286. https://doi.org/10.1016/j.energy.2023.129286
18. Ma, J., Xia, B., & An, Y. (2022). Advanced developments in low-toxic and environmentally friendly shale inhibitor: A review. *Journal of Petroleum Science and Engineering*, *208*, 109578. https://doi.org/10.1016/j.petrol.2021.109578
19. May, P. A., Deville, J. P., & Miller, J. J. (2022). Shale Inhibitor Tracking for High-Performance Water-Based Drilling Fluids. IADC/SPE International Drilling Conference and Exhibition. https://doi.org/10.2118/208721-ms
20. Md. Amanullah, Raed Alouhali and Mohammed K Arfaj (2018): Impact of Geological and Geo-mechanical Controls in Creating Various Drilling Problems. Search and Discovery Online Journal for E&P Geoscientists. AAPG/Data pages Inc., Tulsa, USA, Search & Discovery Article#42199, April 23.
21. Metwally, M. (2024). Advancing ERW Efficiency: Developing High-Performance Water-Based Mud with Friction Reducer and Precision Prediction for ECD and Open Hole Extension Limits using Herschel-Bulkley Rheological Model. Journal of Petroleum and Chemical Engineering, 2(1), 9–19. https://doi.org/10.5281/zenodo.10573628
22. Metwally, M., Nguyen, T. D., Wiggins, H., Saasen, A., & Gipson, M. (2022). Experimental lab approach for water-based drilling fluid using polyacrylamide friction reducers to drill extended horizontal wells. *Journal of Petroleum Science and Engineering*, *212*, 110132. https://doi.org/10.1016/j.petrol.2022.110132.

23. Metwally, M., Nguyen, T., Wiggins, H., Saasen, A., Gipson, M., and H. Yoo. (2023). "Evaluations of Polyacrylamide Water-Based Drilling Fluids for Horizontal Drilling in the Shaly Wolfcamp Formation." SPE J. 28: 1744–1759. doi: https://doi.org/10.2118/214671-PA
24. Metwally, M., & Nguyen, T. (2023). Effectiveness of Shale Inhibition by Anionic and Cationic Polyacrylamide Copolymers in Water Based Mud. The 2023 AADE National Technical Conference and Exhibition, The Bush Convention Center, Midland, Texas. https://doi.org/10.5281/zenodo.10108934
25. Miyashiro, T., & Ruby, E. G. (2012). Shedding light on bioluminescence regulation in Vibrio fischeri. Molecular Microbiology, 84(5), 795–806. https://doi.org/10.1111/j.1365-2958.2012.08065.x
26. Mohamed, Abdelmjeed, Saad Al-Afnan, Salaheldin Elkatatny, and Ibnelwaleed Hussein. (2020). "Prevention of Barite Sag in Water-Based Drilling Fluids by A Urea-Based Additive for Drilling Deep Formations" Sustainability 12, no. 7: 2719. https://doi.org/10.3390/su12072719
27. Morrison, A., Serov, N. A., & Fahmy, A. (2019). Completing Ultra Extended-Reach Wells: Overcoming the Torque and Drag Constraints of Brine. The Abu Dhabi International Petroleum Exhibition & Conference. https://doi.org/10.2118/197678-ms
28. Mpofu, P., Addai-Mensah, J. & Ralston, J. (2004). Temperature influence of nonionic polyethylene oxide and anionic polyacrylamide on flocculation and dewatering behavior of kaolinite dispersions. J. Colloid Interface Sci. , 145–156
29. Murtaza, M., Ahmad, H. M., Kamal, M. S., Hussain, S. M. S., Mahmoud, M., & Patil, S. (2020). Evaluation of Clay Hydration and Swelling Inhibition Using Quaternary Ammonium Dicationic Surfactant with Phenyl Linker. Molecules, 25(18), 4333. https://doi.org/10.3390/molecules25184333
30. Njuguna, J., Siddique, S., Kwroffie, L. B., Piromrat, S., Addae-Afoakwa, K., Ekeh-Adegbotolu, U., Oluyemi, G., Yates, K., Mishra, A. K., & Moller, L. (2022). The fate of waste drilling fluids from oil & gas industry activities in the exploration and production operations. Waste Management, 139, 362–380. https://doi.org/10.1016/j.wasman.2021.12.025
31. Okon, A. N. (2018). Water Coning Prediction: An evaluation of horizontal well correlations. Engineering and Applied Sciences. https://doi.org/10.11648/j.eas.20180301.14
32. Patel, Arvind D. (2009). Design and Development of Quaternary Amine Compounds: Shale Inhibition with Improved Environmental Profile. Paper presented at the SPE International Symposium on Oilfield Chemistry, The Woodlands, Texas. doi: https://doi.org/10.2118/121737-MS
33. Rady, A., May, P., Zhou, H., Deville, J., Miller, J., Metwally, M. (2024). New Shale Inhibitor Tracking Technology for High-Performance Water-Based Drilling Fluids. Paper presented at the AADE 2024 Fluids Technical Conference and Exhibition, Houston, Texas, USA.
34. Rassenfoss, S. (2022). *The trend in drilling horizontal wells is longer, faster, cheaper*. JPT. https://jpt.spe.org/the-trend-in-drilling-horizontal-wells-is-longer-faster-cheaper
35. Sharma, Akash, and Ian Thomasset. (2019). Data-driven Approach to Quantify Oilfield Water Lifecycle and Economics in the Permian Basin. Paper presented at the SPE/AAPG/SEG Unconventional Resources Technology Conference, Denver, Colorado, USA. doi: https://doi.org/10.15530/urtec-2019-968
36. Snee, J. L., & Zoback, M. D. (2018). State of stress in the Permian Basin, Texas and New Mexico: Implications for induced seismicity. *The Leading Edge*, *37*(2), 127–134.
37. Stefano, G., and S. Young. (2009). "The Prevention And Cure Of Bit Balling In Water Based Drilling Fluids." Paper presented at the Offshore Mediterranean Conference and Exhibition, Ravenna, Italy.
38. Sun, H., Stevens, R. F., Cutler, J., Wood, B., Wheeler, R. S., & Qu, Q. (2010). A novel Nondamaging Friction Reducer: Development and Successful Slickwater FRAC applications. *All Days*. https://doi.org/10.2118/136806-ms
39. Varnaseri, M., Peyghambarzadeh, S.M. (2020). The effect of polyacrylamide drag reducing agent on friction factor and heat transfer coefficient in laminar, transition and turbulent flow regimes in circular pipes with different diameters. Int. J. Heat Mass Tran. 154, 119815. https://doi.org/10.1016/j. ijheatmasstransfer.2020.119815
40. Ward, Robert F, Kendall, Christopher G St C, and Harris, Paul M. (1986). Upper Permian (Guadalupian) facies and their association with hydrocarbons—Permian Basin, west Texas and New Mexico. AAPG bulletin 70 (3): 239–262. doi: https://doi.org/10.1306/9488566F-1704-11D7-8645000102C1865D
41. Willis, John, Tellez, Diego, Neel, Randy et al. (2018). Unconventional Drilling in the New Mexico Delaware Basin Case History. Proc., IADC/SPE Drilling Conference and Exhibition. https://doi.org/10.2118/189597-MS
42. Xiong, B., Loss, R. D., Shields, D., Pawlik, T., Hochreiter, R., Zydney, A. L., & Kumar, M. (2018). Polyacrylamide degradation and its implications in environmental systems. Npj Clean Water, 1(1). https://doi.org/10.1038/s41545-018-0016-8
43. Zamora, M., Bell, R. (2004). Improved wellsite test for monitoring barite sag. AADE 2004 Drilling Fluids Conference, held at the Radisson Astrodome in Houston, Texas.
44. Zhang, J. J. (2019). Applied Petroleum Geomechanics. Gulf Professional Publishing.